

---

# State-of-Charge and State-of-Health prediction of Lead-acid Batteries for Hybrid Electric Vehicles using non-linear observers

B.S. Bhangu, P. Bentley, D.A. Stone and C.M. Bingham  
UNIVERSITY OF SHEFFIELD  
Department of Electronic and Electrical Engineering,  
University of Sheffield, Mappin Street,  
Sheffield, S1 3JD, UK.  
Tel.: +44 / (0) – 1142225195  
Fax: +44 / (0) – 1142225196  
E-Mail: [b.bhangu@sheffield.co.uk](mailto:b.bhangu@sheffield.co.uk)  
URL: <http://www.sheffield.ac.uk>

## Acknowledgements

The authors wish to acknowledge the financial assistance provided by the UK's DTI Foresight Vehicle Link Program, and the EPSRC, who have funded the RHOLAB project jointly with the European Advanced Lead Acid Battery Consortium, and Hawker Batteries. They would also like to acknowledge the support given by the other partners in the project, namely, Provector Ltd, the University of Warwick and Hawker Batteries (now part of Enersys Inc.).

## Keywords

Battery management systems (BMS), Energy storage, Estimation technique, Hybrid electric vehicle (HEV), Modelling

## Abstract

The paper describes the application of state-estimation techniques for the real-time prediction of state-of-charge (SoC) and state-of-health (SoH) of lead-acid cells. Approaches based on the Extended Kalman Filter (EKF) are presented to provide correction for offset, drift and state divergence—an unfortunate feature of more traditional coulomb-counting techniques. Experimental results are employed to demonstrate the relative attributes of the proposed methodology.

## Introduction

Peak power buffers of hybrid electric vehicles (HEVs) are, by their very nature, subject to large dynamic transients in current and power demand. Road data collected from a Honda Insight HEV (RHOLAB driving cycle [1]), where peak charge- and discharge-current demands of  $\approx 60\text{A}$  and  $\approx 100\text{A}$ , respectively, are required from the battery pack when subjected to a series of vehicle driving tests [1]. The accommodation of such operating conditions requires that the management system have accurate knowledge of the peak power buffer's SoC to facilitate safe and efficient operation. Failure to control SoC will ultimately lead to under- or over-charging conditions, which can degrade the ability of the pack to source/sink subsequent power transients.

A variety of techniques have been proposed to measure or monitor the SoC of a cell or battery, with charge counting or current integration at present being the most commonly used technique. However, due to the reliance on integration, errors in terminal measurements due to noise, resolution and rounding are

cumulative, and large SoC errors can result. Furthermore, manufacturers of HEVs would like predictions of the State-of-Health (SoH) or State-of-Function (SoF) of a battery pack, since the increasing reliance on drive-by-wire technologies is making the battery a key safety-critical component of the vehicle. Knowledge of whether a battery will fail when subject to high transient loadings, as may be experienced in emergency braking, for instance, is therefore essential. However, SoH monitoring techniques are currently in their infancy, with little being reported to-date.

Here then, model-based state-estimation techniques are proposed for predicting states of a cell that would normally be difficult or expensive to measure. Measurements using real-time road data are used to compare the performance of conventional integration-based methods for estimating SoC, with those predicted from the presented state estimation schemes. Results show that the proposed methodologies are superior to more traditional techniques, with accuracy in determining the SoC within 2%, being demonstrated. Moreover, by accounting for the nonlinearities present within the dynamic cell model, the application of an EKF is shown to provide verifiable indications of SoH of the cell pack via the real-time state estimation. Experimental results ultimately show the ability of the EKF to track changes and to compensate for inaccuracies in the initial estimates of cell model bulk capacitance, that can be considered as a measure of the cell's capacity.

## Battery Model

A dynamic model of the battery, in the form of state variable equations, is necessary to predict the SoC or SoH. Here, a generic model [2] consisting of a bulk capacitor,  $C_{bulk}$ , to characterise the ability of the battery to store charge, a capacitor to model surface capacitance and diffusion effects within the cell  $C_{surface}$ , a terminal resistance  $R_t$ , surface resistance  $R_s$  and end resistance,  $R_e$  is employed as shown by Fig.1. The voltage across the bulk- and surface- capacitors are denoted  $V_{Cb}$  and  $V_{Cs}$ , respectively.

The cell tested in this paper is a novel, spiral wound, 8Ah sealed lead-acid cell, with terminals on either end, developed by Hawker (ENERSYS Inc), Fig. 2. The double terminal encapsulation is introduced to lower grid currents, and hence, thermal gradients, and thereby promote efficient utilization of the active materials in the cell, thus leading to a battery that is optimised for the high-power duties typical of hybrid driving cycles.

Initial parameters of the cell, Fig. 1, are pre-calculated from experimental data, where open-circuit voltage (OCV) tests are performed upon successive discharges of the battery, by injection of current pulses. An initial estimate of  $C_{bulk}$  is obtained by analyzing the amount of stored energy in the cell (from SoC = 1 to SoC = 0), to a discharge current pulses of 1.53A, applied for  $t=1800s$ , every 3600s interval. Note that SoC = 1 is a normalized value used to define a fully-charged cell. The provisional value of  $C_{surface}$  relies on

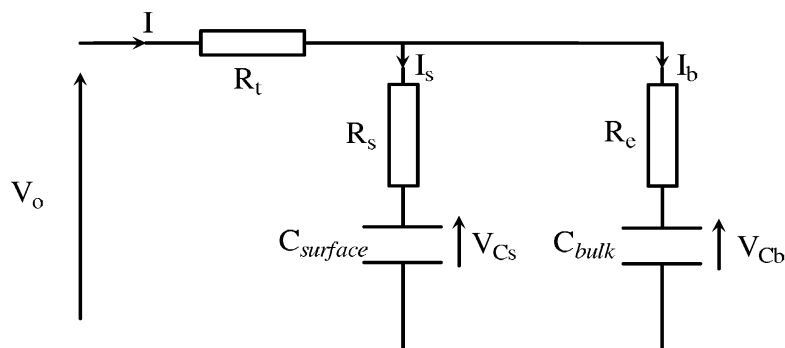


Fig. 1: RC Battery model schematic



Fig. 2: 8Ah sealed lead-acid test cell

calculating the time-constant of the cell in response to high frequency excitation, by subjecting discharge pulses of 10A, at 500ms intervals, thereby isolating the results from the effects of  $C_{bulk}$ . The internal resistance of the battery is measured as  $4.6m\Omega$  and it is assumed that  $R_e$  and  $R_s$  are equivalent and account for 75% of total resistance. The complete initial parameters for the cell considered, is provided by Table I.

**Table I: Parameters for cell model**

$C_{bulk}$	88372.83 F
$C_{surface}$	82.11 F
$R_e$	0.00375 $\Omega$
$R_c$	0.00375 $\Omega$
$R_t$	0.002745 $\Omega$

## State variable description of the battery model

The characteristics of the network shown in Fig. 1, are given by (note: by convention, current flowing into the cell is considered positive):

$$\begin{aligned} V_0 &= IR_t + I_b R_e + V_{C_{bulk}} \\ V_0 &= IR_t + I_s R_s + V_{C_{surface}} \end{aligned} \quad (1)$$

Equating the two voltage equations and noting that:

$$\begin{aligned} I_b &= \dot{V}_{Cb} C_{bulk} \\ I_s &= \dot{V}_{Cs} C_{surface} \end{aligned} \quad (2)$$

a complete state variable description of the network relating the voltages and currents, is obtained as shown by (3). However, note the third state is obtained by taking the time-derivative of the output voltage, and assuming  $dl/dt \approx 0$  (the rate of change of terminal current, per sampling interval when implemented digitally, is negligible).

$$\begin{bmatrix} \dot{V}_{Cb} \\ \dot{V}_{Cs} \\ \dot{V}_0 \end{bmatrix} = \begin{bmatrix} -\frac{1}{C_{bulk}R_\lambda} & \frac{1}{C_{bulk}R_\lambda} & 0 \\ \frac{1}{C_{surface}R_\lambda} & -\frac{1}{C_{surface}R_\lambda} & 0 \\ A(3,1) & 0 & A(3,3) \end{bmatrix} \begin{bmatrix} V_{Cb} \\ V_{Cs} \\ V_0 \end{bmatrix} + \begin{bmatrix} \frac{R_s}{C_{bulk}R_\lambda} \\ \frac{R_e}{C_{surface}R_\lambda} \\ \frac{R_e^2}{C_{surface}R_\lambda^2} - \frac{R_s R_t}{C_{bulk}R_e R_\lambda} + \frac{R_t}{C_{surface}R_\lambda} + \frac{R_e R_s}{C_{surface}R_\lambda^2} \end{bmatrix} I$$

$$\begin{aligned}
A(3,1) &= -\frac{R_s}{C_{bulk}R_\lambda^2} + \frac{R_e}{C_{surface}R_\lambda^2} - \frac{R_s^2}{C_{bulk}R_eR_\lambda^2} + \frac{R_s}{C_{surface}R_\lambda^2} \\
A(3,3) &= \frac{R_s}{C_{bulk}R_eR_\lambda^2} - \frac{1}{C_{surface}R_\lambda}
\end{aligned} \tag{3}$$

where  $R_\lambda = R_e + R_s$ .

Assuming, for now, that cell parameters are time invariant quantities, the recursive KF algorithm, Fig. 3, is applied, where an equivalent discrete-time model of (3) is obtained by using Euler transformation.

$$\mathbf{A}_d = \begin{bmatrix} 1 - \frac{T_c}{C_{bulk}R_\lambda} & \frac{T_c}{C_{bulk}R_\lambda} & 0 \\ \frac{T_c}{C_{surface}R_\lambda} & 1 - \frac{T_c}{C_{surface}R_\lambda} & 0 \\ A_d(3,1) & 0 & A_d(3,3) \end{bmatrix}$$

$$\mathbf{B}_d = \begin{bmatrix} \frac{T_c R_s}{C_{bulk} R_\lambda} \\ \frac{T_c R_e}{C_{surface} R_\lambda} \\ \frac{T_c R_e^2}{C_{surface} R_\lambda^2} - \frac{T_c R_s R_t}{C_{bulk} R_e R_\lambda} + \frac{T_c R_t}{C_{surface} R_\lambda} + \frac{T_c R_e R_s}{C_{surface} R_\lambda^2} \end{bmatrix}$$

$$\mathbf{C}_d = \mathbf{C}$$

where

$$\begin{aligned}
A_d(3,1) &= -\frac{T_c R_s}{C_{bulk} R_\lambda^2} + \frac{T_c R_e}{C_{surface} R_\lambda^2} - \frac{T_c R_s^2}{C_{bulk} R_e R_\lambda^2} + \frac{T_c R_s}{C_{surface} R_\lambda^2} \\
A_d(3,3) &= 1 + \frac{T_c R_s}{C_{bulk} R_e R_\lambda^2} - \frac{T_c}{C_{surface} R_\lambda}
\end{aligned} \tag{4}$$

## Comparison of State of Charge estimation technique

The stochastic principles underpinning the Kalman Filter (KF) are appealing for this investigation, since it is recognised that the presence of disturbances stemming from sensor noise on the cell terminal measurements, and the use of non-ideal dynamic models, make it impossible to predict with certainty the states of the system over prolonged time periods—a statistical predictor/corrector formulation thereby providing obvious advantages. Here then, KF is applied, Fig. 3, to the real-time estimation of SoC of a single cell that is subject to a RHOLAB driving cycle [1], see Fig. 4. Since only terminal quantities of the battery can be measured, the input is defined as  $u = I$ , and the measured output is  $y = V_0$ . The initial cell SoC is set to 0.8, this being the defined operating point for partial SoC on the HEV driving profile.

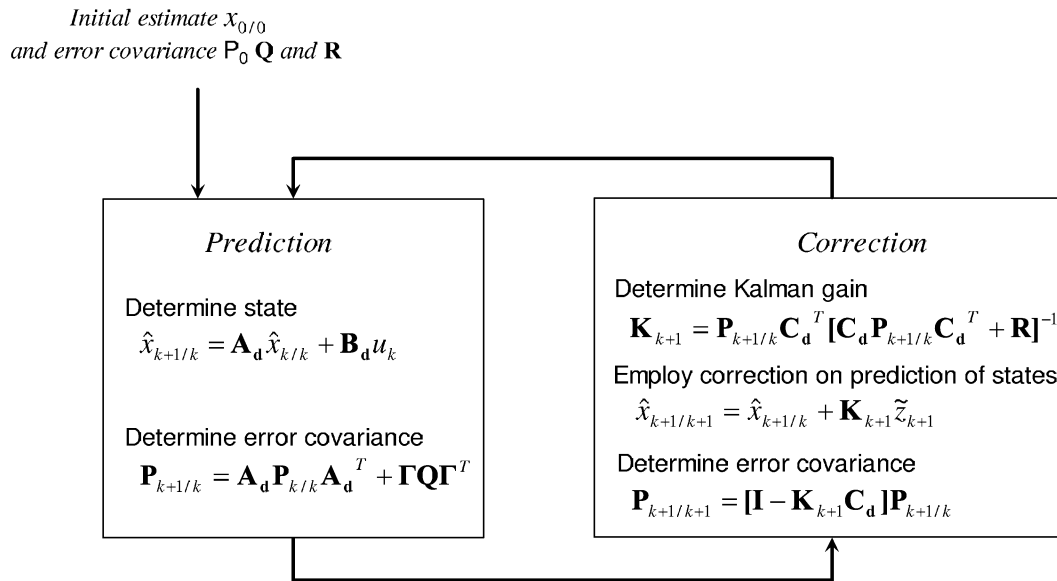


Fig. 3: Recursive Kalman Filter algorithm

Upon subjecting the cell to the RHOLAB driving cell-current profile, excellent convergence of the estimated output voltage from the KF is seen with negligible error ( $< \pm 0.05$  V), Fig. 5(a). Figure 5(b) shows the estimated bulk and surface capacitor voltages. Furthermore, results using conventional SoC estimation, by the integration of current method, with charging efficiency fixed at 0.97 [1], and those from the proposed KF scheme, are given in Fig. 6. Having been subjected to a RHOLAB driving cycle, at  $t=1400$ s, the tests are terminated, and the remnant charge in the cell is measured using a 1.53A discharge, to a terminal voltage of 1.7V, and noting the remaining Ampere-hours. This corresponds to a final SoC of the cell of 0.167. From Fig. 6, it can be seen that the performance of the KF is excellent, and, although both SoC estimation techniques follow the correct profile, the integration-based method demonstrates significant drift over time, with an error of  $\approx 15\%$  ensuing, whereas the KF consistently provides estimates within  $\approx 2\%$  of the measured values.

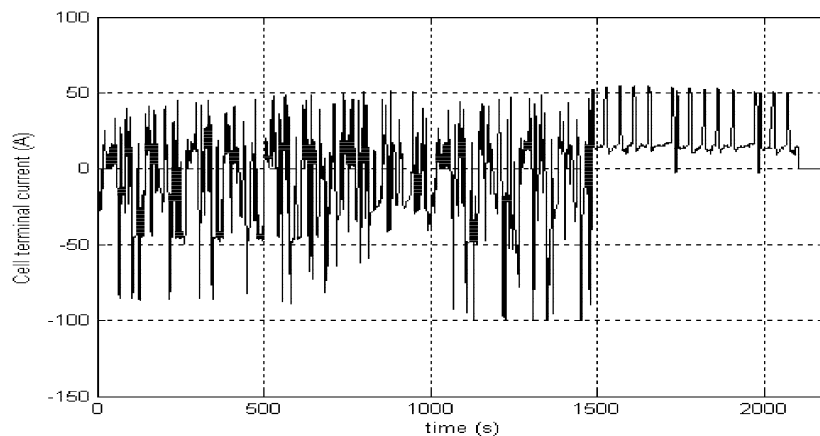


Fig. 4: Typical RHOLAB [1] driving cycle cell current

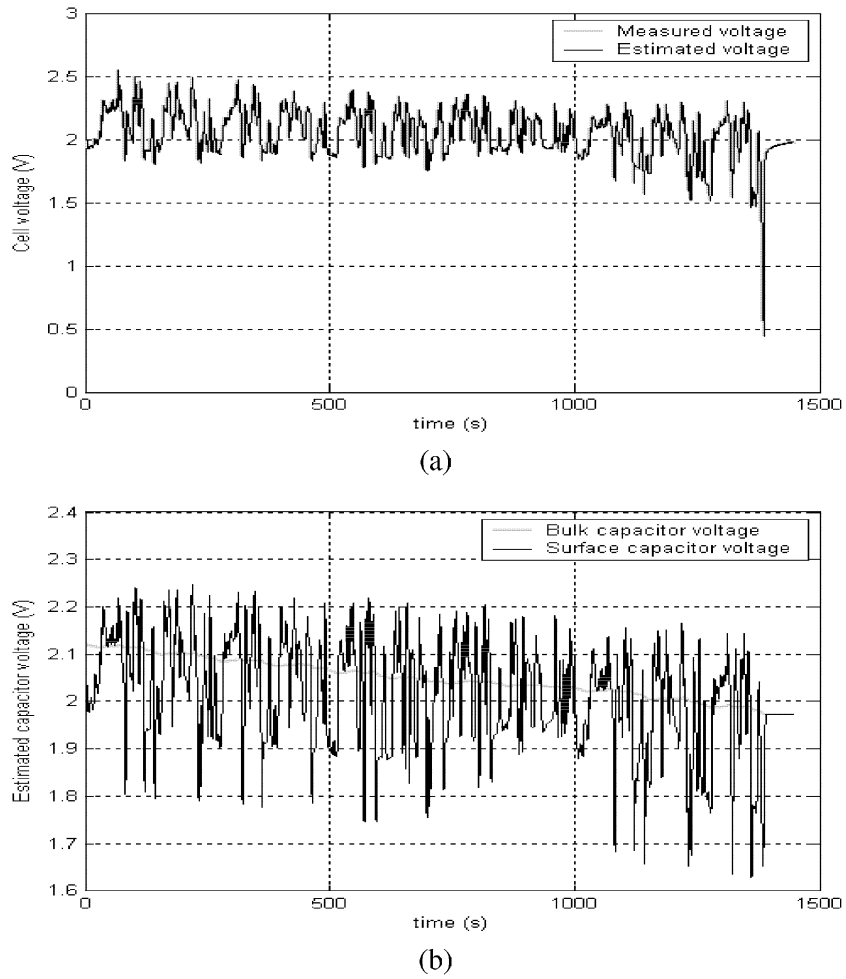


Fig. 5: Implementation of KF on RHOLAB cycle (a) measured and estimated cell voltage (b) estimated bulk and surface capacitor voltage

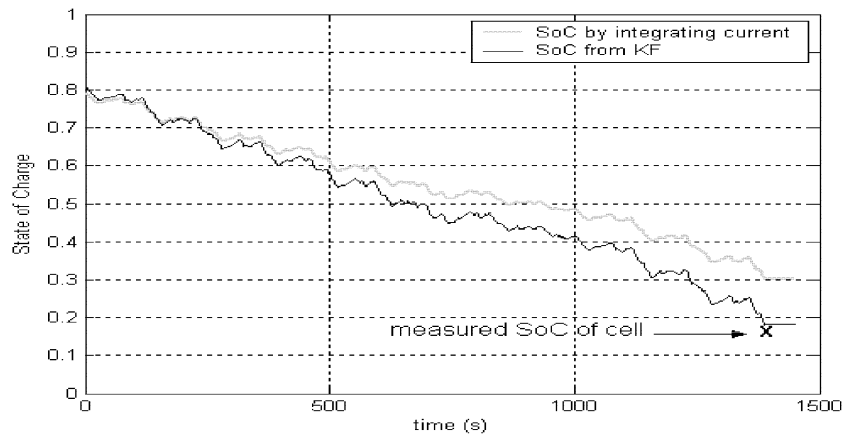


Fig. 6: Comparison of determination of SoC by conventional means by integration of current and from estimated bulk capacitor voltage

## Estimation of State of Health of cell

SoH is the ability of a cell to store energy, source and sink high currents and retain charge over extended periods, relative to its initial or nominal capabilities. The available charge stored within a fully-charged cell is expected to fall with cell usage. Such capacity-loss mechanisms generally occur slowly in VRLA batteries that are cycled at low-rates over their full SoC range. However, when operated as a peak power buffer, in a HEV system, the cells are operated at a Partial State-of-Charge (PSoC) i.e. the cell is never cycled over its full SoC range, and is subjected to both high charge and discharge currents. Studies have shown that this PSoC operation can lead to truncated service life in VRLA cells [3,4]. Such capacity loss can be deemed a loss of cell SoH. Early detection of SoH degradation would allow a ‘smart’ battery pack to take remedial action, such as the application of conditioning routines to the cell, to remove small sulphate crystals before they form large inactive crystals, thereby restoring the cells capacity. Measuring cell capacity by the standard means of a low current discharge is impractical for HEV applications, and online techniques that utilise only cell terminal measurements, made whilst the HEV is driven, are therefore required.

Here, a proposed means of estimating bulk capacitance  $C_{bulk}$ , by adding an extra state,  $dC_{bulk}/dt = 0$ , into the observer structure, is demonstrated. Since the derivatives of  $V_{Cb}$  and  $V_0$  are now coupled by non-linear elements, an EKF is required for effective estimation of state variables. However, note that the proposed realisation results in an increase in order of the Jacobians, covariance, noise and disturbance matrices, with a consequential increase in computation overhead. The proposed non-linear battery model is written in the form:

$$\begin{aligned} \dot{x} &= f(x, u) \\ y &= C(x) \end{aligned} \quad (5)$$

where  $f(x, u)$  is given by (6)

$$x = [V_{Cb}, V_{Cs}, V_0, \alpha]^T, \quad f(x, u) = \begin{bmatrix} -\frac{V_{Cb}\alpha}{R_\lambda} + \frac{V_{Cs}\alpha}{R_\lambda} + \frac{IR_s\alpha}{R_\lambda} \\ \frac{1}{C_{surface}} \left[ \frac{V_{Cb}}{R_\lambda} - \frac{V_{Cs}}{R_\lambda} + \frac{IR_e}{R_\lambda} \right] \\ V_{Cb} \cdot f1 + V_0 \cdot f2 + I \cdot f3 \\ 0 \end{bmatrix},$$

$$\begin{aligned} f1 &= -\frac{R_s\alpha}{R_\lambda^2} + \frac{R_e}{C_{surface}R_\lambda^2} - \frac{R_s^2\alpha}{R_eR_\lambda^2} + \frac{R_s}{C_{surface}R_\lambda^2} \\ f2 &= -\frac{R_s\alpha}{R_eR_\lambda} - \frac{1}{C_{surface}R_\lambda} \\ f3 &= \frac{R_e^2}{C_{surface}R_\lambda^2} - \frac{R_sR_t\alpha}{R_eR_\lambda} + \frac{R_t}{C_{surface}R_\lambda} + \frac{R_eR_s}{C_{surface}R_\lambda^2} \end{aligned}$$

$$\text{where } C(x) = V_0, \quad \alpha = 1/C_{bulk}, \quad \text{and } R_\lambda = R_e + R_s. \quad (6)$$

Here, the EKF requires a small-signal model of the system, at each sample step, about the current operating point,  $x_0$ ,  $u_0$  and is given by:

$$\delta\dot{x} = \mathbf{A}_k \delta x + \mathbf{B}_k \delta u, \quad \delta y = \mathbf{C} \delta x \quad (7)$$

where  $\mathbf{A}_k = \mathbf{F}(x) \Big|_{x_k, u_k}$  and is defined by (8):

$$\mathbf{F}(x) = \frac{\partial f}{\partial x} \Big|_{x(t), u(t)} = \begin{bmatrix} -\frac{\alpha}{R_\lambda} & \frac{\alpha}{R_\lambda} & 0 & F(1,4) \\ \frac{1}{C_{surface} R_\lambda} & -\frac{1}{C_{surface} R_\lambda} & 0 & 0 \\ F(3,1) & 0 & \frac{R_s \alpha}{R_e R_\lambda} - \frac{1}{C_{surface} R_\lambda} & F(3,4) \\ 0 & 0 & 0 & 0 \end{bmatrix}$$

$$F(1,4) = -\frac{V_{Cb}}{R_\lambda} + \frac{V_{Cs}}{R_\lambda} + \frac{R_s I}{R_\lambda}$$

$$F(3,1) = -\frac{R_s \alpha}{R_\lambda^2} + \frac{R_e}{C_{surface} R_\lambda^2} - \frac{R_s^2 \alpha}{R_e R_\lambda^2} + \frac{R_s}{C_{surface} R_\lambda^2}$$

$$F(3,4) = -\frac{V_{Cb} R_s}{R_\lambda^2} - \frac{V_{Cb} R_s^2}{R_e R_\lambda} + \frac{V_0 R_s}{R_e R_\lambda} - \frac{R_s R_t I}{R_e R_\lambda}$$

$$\mathbf{B} = \frac{\partial f}{\partial u} \Big|_{x(t), u(t)} = \begin{bmatrix} \frac{R_s \alpha}{R_\lambda} & \frac{R_e}{C_{surface} R_\lambda} & f_3 & 0 \end{bmatrix}^T$$

$$\mathbf{C} = \frac{\partial C}{\partial x} \Big|_{x(t), u(t)} = [0 \quad 0 \quad 1 \quad 0] \quad (8)$$

that can be discretized, to give (9) and used in the KF algorithm described previously in Fig. 3.:

$$\begin{aligned} x_{k+1} &= \mathbf{A}_d x_k + \mathbf{B}_d u_k \\ y_{k+1} &= \mathbf{C}_d x_{k+1} \end{aligned} \quad (9)$$

The SoH of known cells has previously been evaluated [3] by performing continuous power cycling tests (using the RHOLAB profile shown in Fig. 4), and during the tests, the cells suffered a measured loss of capacity of  $\approx 0.77$  Ah [3]. Whilst performing the tests, the EKF is employed, and the variation of  $C_{bulk}$  is estimated, Fig. 7(a), and ultimately over time indicates a reduction of  $\approx 10\%$  during the tests, corresponding to an average loss of cell capacity of  $\approx 0.8$  Ah for a nominal 8 Ah cell- hence comparing well with the measured loss of capacity. Figure 7(b), shows the voltage profile over the continuous power cycling test.



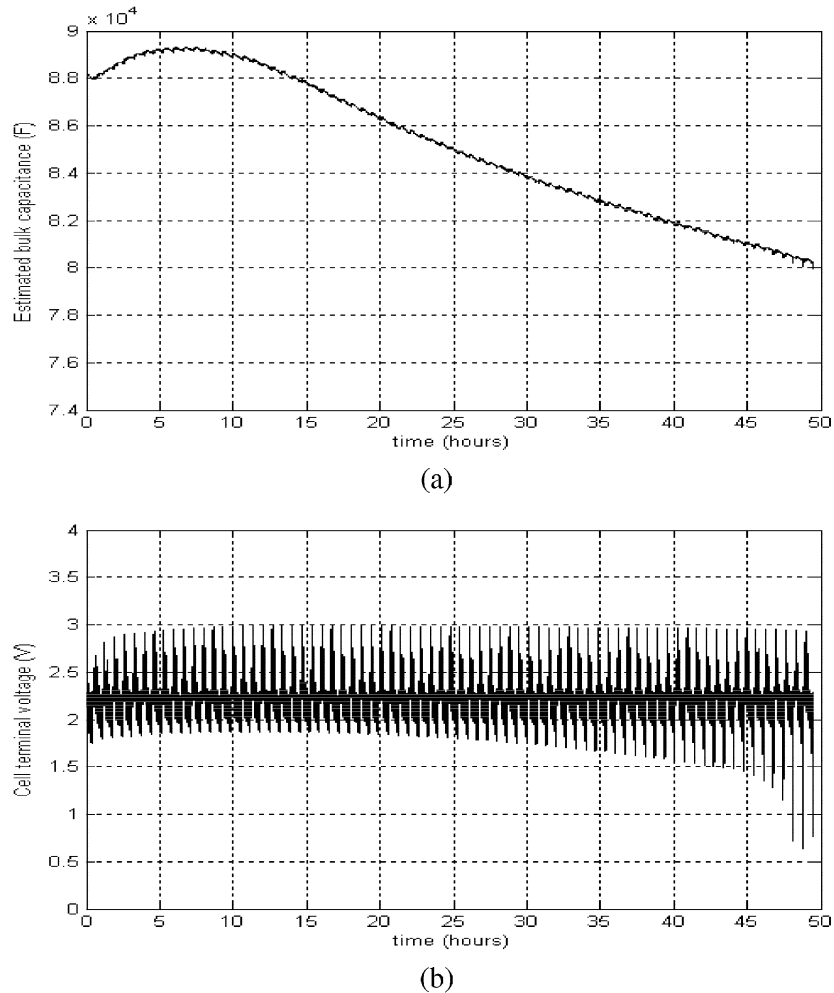


Fig. 7: On-line EKF employed to predict SoH of cell pack (a) estimated bulk capacitance  $C_{bulk}$  (b) cell terminal voltage

## Conclusion

This paper presents an alternative approach to estimating the SoC of a cell pack by implementation of observer-based techniques. Using generic models like the one presented to describe the dynamic behaviour of lead-acid cells, large state errors and divergence ensue when estimating SoC. However, rather than increasing the complexity of the cell model to closely match the real system, the application of a KF, with its inherent predictor-corrector mechanism, is shown to accommodate such inadequacies. In particular, a comparison of SoC estimates using the presented KF technique, and the more conventional integration of current method, is undertaken using “road data” collected from a Honda Insight HEV driven on a test track. The presented results show a significant improvement in SoC estimation from the proposed KF methodology, when compared to the more traditional current integration method. Furthermore, extensions for SoH on-line monitoring, by employing an EKF is also presented—using only measurements of cell terminal quantities as input.

Ultimately, the complete HEV Smart VRLA battery pack will consist of a series of cells, cascaded together in a module. However, within the module, one cell is always out of circuit, hereby allowing active conditioning routines to be applied, hence the module consists of  $n+1$  cells ( $n$  being the series string length). Knowledge of SoC and SoH of each individual cell obtained from the observer will allow the

selection of cell most in need of conditioning and the chosen cell is automatically taken out of the series string. Such control of the Smart VRLA module will significantly increase the lifetime of the cells for HEV demands. Furthermore, from a manufacturers perspective, such data is extremely important for the ultimate prediction of State-of-Function (SoF), which describes the ability of a cell to perform adequately under HEV demands. SoF will give a prediction of available capacity, and discharge and recharge capability, thereby allowing Smart VRLA module to forecast the response of each cell to driving demands, and leading to optimal utilisation of the battery pack with regard to performance and lifetime, and therefore, better overall energy management within the vehicle.

## References

- [1] M. J. Kellaway, P. Jennings, D. Stone, E. Crowe, and A. Cooper, "Early results from a systems approach to improving the performance and lifetime of lead acid batteries," *J. Power Sources*, vol. 116, pp. 110–117, 2003.
- [2] V. H. Johnson, A. A. Pesaran, and T. Sack, "Temperature-dependent battery models for high-power lithium-ion batteries," presented at the Proc. EVS 17, Montreal, PQ, Canada, 2000.
- [3] P. Bentley and D. A. Stone, "Lifetime extension of Valve regulated lead acid (VRLA) batteries under hybrid vehicle duty," in Proc. 2<sup>nd</sup> Int. Power Electronics Machines and Drives Conf. (PEMD'04), vol. 1, Edinburgh, U.K., pp. 49–54, 2004.
- [4] Hollenkamp, Baldsing, Lim et al. "Overcoming negative-plate capacity loss in VRLA batteries cycled under partial state-of-charge duty," ALABC Investigation report ET/IR398R, 2001.